Calcolo (2012) 49:193–219
DOI 10.1007/s10092-011-0051-z

Computation of the signed distance function to a discrete contour on adapted triangulation

Charles Dapogny · Pascal Frey

Received: 6 May 2011 / Accepted: 7 December 2011 / Published online: 5 January 2012

Abstract In this paper, we propose a numerical method for computing the signed distance function to a discrete domain, on an arbitrary triangular background mesh. It mainly relies on the use of some theoretical properties of the unsteady Eikonal equation. Then we present a way of adapting the mesh on which computations are held to enhance the accuracy for both the approximation of the signed distance function and the approximation of the initial discrete contour by the induced piecewise affine reconstruction, which is crucial when using this signed distance function in a context of level set methods. Several examples are presented to assess our analysis, in two or three dimensions.

Keywords Signed distance function · Eikonal equation · Level set method · Anisotropic mesh adaptation · $\mathbb{P}^1$-finite elements interpolation

Mathematics Subject Classification (2000) 65M25 · 65M50 · 35F20

1 Introduction

The knowledge of the signed distance function to a domain $\Omega \subset \mathbb{R}^d$ ($d = 2, 3$ in our applications) has proved a very valuable information in various fields such as collision

The first author is partially supported by the Chair "Mathematical modelling and numerical simulation, F-EADS, Ecole Polytechnique, INRIA".

C. Dapogny (✉)
Centre de Mathématiques Appliquées (UMR 7641), Ecole Polytechnique 91128 Palaiseau, France
e-mail: dapogny@ann.jussieu.fr

C. Dapogny
Renault DREAM-DTAA, Guyancourt, France

P. Frey
Laboratoire J.-L. Lions, UPMC Univ Paris 06, UMR 7598, 75005 Paris, France

detection [19], shape reconstruction from an unorganized cloud of points [11, 43], and of course when it comes to level set methods, introduced by Sethian and Osher [33] (see also [37] or [32] for multiple topics around the level set method), where ensuring the property of unitary gradient of the level set function is especially relevant.

We intend here to devise a numerical algorithm that allows the computation of the signed distance function to a *polyhedral* domain Ω, with minimal assumptions or requirements. We only rely on the knowledge of a triangular mesh $\mathcal{S}$ of its boundary $\partial\Omega$, which we suppose orientable (if not, the interior Ω is ill-defined on the sole basis of its boundary). Making this assumption, we imply here that we do not rely on any knowledge of the exterior normal to the surface, nor do we suppose the mesh $\mathcal{S}$ to be conformal. We do not want to make any kind of assumption on the triangular background mesh $\mathcal{T}$ on which the computations are performed either, even if, of course, the quality of the solution may depend on it, as will be seen.

Regarding the computation of the signed distance function, there exist mainly two types of approaches, both of them being based on an approximation of the solution of the Eikonal equation (1). The first one consists in treating this equation as a stationary boundary value problem, starting from the knowledge of the distance in the elements of the computational grid or mesh which are close to the interface $\partial\Omega$, and propagating the information throughout the whole domain. The most notorious methods—such as the Fast Marching Method [26, 35, 36] or the Fast Sweeping Method [42], [31]—belong to this category, and rely on a local solver for the Eikonal equation, and on a marching method, meant to enforce the natural causality embedded in the equation. Another way of addressing the problem is to consider it as an unsteady problem and then to devise a propagation method for extending the signed distance field from the boundary of Ω—see [8, 39, 40]. This is the point of view which is at stake in this paper. This leads to an efficient, easy to implement, and easy to parallelize method for computing the signed distance function to Ω. The proposed method is presented in dimensions 2 and 3, but naturally extends to the general case.

What is more, when we want to use the signed distance function as an implicit function defining the initial domain Ω from which we intend to evolve, the discrete interface obtained as the 0 level set of the discrete signed distance function can turn out to be quite different from the true interface $\partial\Omega$. Following the work presented in [15], we intend here to present an adaptation scheme, based on the signed distance function, to produce a background mesh adapted to the boundary $\partial\Omega$ so as to improve in the meantime, the computation of the signed distance function to Ω—at least in the areas of the computational domain where it is relevant—and the discrete numerical reconstruction of Ω.

The remainder of this paper is organized as follows. In Sect. 2, we review some general properties of the signed distance function, and among other things recall how it can be seen as the stationary state of the solution of the unsteady Eikonal equation, which leads us to studying the dynamics of this equation in Sect. 3. From this study, we infer a numerical scheme for approximating the signed distance function in Sect. 4. We then show in Sect. 5.1 how the background triangular mesh on which the computation is held can be adapted so that both the approximation of the signed distance function and the discrete isosurface resulting from the process can be controlled and improved. We briefly discuss two interesting extensions of this work, to the problem of reinitialization of a level set function in Sect. 6, and to the computation of the signed distance function to a domain in a Riemannian space in Sect. 7. Numerical examples are eventually provided in Sect. 8 to emphasize the main features of our approach.

2 Some preliminaries about the signed distance function

So as to get a better intuition about the signed distance function and the various difficulties it raises, let us briefly recall some 'classical' results around the topic.

Definition 1 Let $\Omega \subset \mathbb{R}^d$ a bounded domain. The *signed distance function* to Ω is the function $\mathbb{R}^d \ni x \mapsto u_\Omega(x)$ defined by:

$$u_\Omega(x) = \begin{cases} -d(x, \partial\Omega) & \text{if } x \in \Omega, \\ 0 & \text{if } x \in \partial\Omega, \\ d(x, \partial\Omega) & \text{if } x \in {}^c\overline{\Omega}, \end{cases}$$

where $d(., \partial\Omega)$ denotes the usual Euclidean distance function to the set $\partial\Omega$.

When studying the distance to such a bounded domain Ω, the fundamental notion of *skeleton* plays a major role:

Definition 2 The *skeleton* of $\partial\Omega$ is the set of points $x \in \mathbb{R}^d$ such that the minimum in

$$d(x, \partial\Omega) = \min_{y\in\partial\Omega} \|x - y\|$$

is achieved for at least two distinct points of $\partial\Omega$.

Being 1-Lipschitz, and owing to Rademacher's theorem [16], the function u_Ω is almost everywhere differentiable. Actually, the following interesting proposition delivers a geometric characterization of the regularity of u_Ω [14].

Theorem 1 *Let $\Omega \subset \mathbb{R}^d$ be a bounded open set with smooth boundary; then u_Ω is smooth in a tubular neighbourhood U of $\partial\Omega$. Moreover, for any point $x \in \mathbb{R}^d$,*

- *either $x \in \partial\Omega$, and then u_Ω is differentiable at x, with*

$$\nabla u_\Omega(x) = n(x), \text{the unit normal vector to } \partial\Omega \text{ at } x$$

- *or $x \in \mathbb{R}^d \setminus \partial\Omega$, then u_Ω is differentiable at x if and only if x belongs to the complementary of the skeleton of $\partial\Omega$. In such a case, there exists a unique point $p_x \in \partial\Omega$ such that $d(x, \partial\Omega) = \|p_x - x\|$, and the gradient of u_Ω at x reads*

$$\nabla u_\Omega(x) = \frac{p_x - x}{u_\Omega(x)}.$$

In particular, u_Ω satisfies the so-called Eikonal equation at every point x where it is differentiable:

$$\|\nabla u_\Omega(x)\| = 1. \tag{1}$$

Unfortunately, theory happens to be scarce as for functions being solutions of a PDE almost everywhere. For this reason—and many others—it is much more convenient from a theoretical point of view to see u_Ω as a *viscosity solution* of the Eikonal equation (see [16] again).

Proposition 1 *u_Ω is a solution of the Eikonal equation* (1) *in the sense of viscosity.*

For the sake of completeness, let us mention that several approaches exist when it comes to studying the very degenerated equation (1); further developments lead to taking into account the boundary condition

$$u_\Omega(x) = 0 \quad \text{on } \partial\Omega$$

in the sense of viscosity (see [12]), but even so, (1) turns out to get 'too much solutions'.

Another way of thinking of u_Ω consists of seeing it as the result of a propagation by means of an evolution equation: suppose Ω is implicitly known as

$$\Omega = \left\{x \in \mathbb{R}^d; u_0(x) < 0\right\} \quad \text{and} \quad \partial\Omega = \left\{x \in \mathbb{R}^d; u_0(x) = 0\right\}, \tag{2}$$

where u_0 is a continuous function. Note that, in the theoretical framework, such a function u_0 exists and is quite easy to construct by means of partitions of unity techniques. Then the function u_Ω can be considered as the steady state of the so-called *redistancing equation* or *unsteady Eikonal equation*

$$\begin{cases} \frac{\partial u}{\partial t} + sgn(u_0)(\|\nabla u\| - 1) = 0 & \forall t > 0, x \in \mathbb{R}^d \\ u(t = 0, x) = u_0(x) & \forall x \in \mathbb{R}^d. \end{cases} \tag{3}$$

Formally speaking, this equation starts with an arbitrary (continuous) function u_0 implicitly defining the domain Ω and straightens it to the "best" function which suits that purpose—u_Ω. For this reason, this equation was first introduced in [41] for redistancing a very stretched level set function arising in a calculus. The following important theorem (a proof can be found in [5] and [24]) makes these statements more precise:

Theorem 2 *Let Ω a bounded domain of $\mathbb{R}^d$ implicitly defined by a continuous function u_0 such that* (2) *holds. Define function u, $\forall x \in \mathbb{R}^d$, $\forall t \in \mathbb{R}_+$,*

$$u(t, x) = \begin{cases} sgn(u_0(x)) \inf_{\|y\| \le t} (sgn(u_0(x)) u_0(x + y) + t) & \text{if } t \le d(x, \partial\Omega) \\ sgn(u_0(x)) d(x, \partial\Omega) & \text{if } t > d(x, \partial\Omega). \end{cases} \tag{4}$$

Let $T \in \mathbb{R}_+$. Then u is the unique uniformly continuous viscosity solution of (3) *such that, for all $0 \le t \le T$, $u(t, x) = 0$ on $\partial\Omega$.*

Note that the exact formula (4) expresses the idea of a propagation of information from the boundary with constant unit speed. This feature will later be exploited to devise our numerical algorithm for computing the signed distance function to Ω.

3 A short study of some properties of the solution to the unsteady Eikonal equation

So as to build a resolution scheme for the unsteady Eikonal equation (3), let us take a closer look to its dynamic in view of the previous section.

The main idea is to start with a function u_0 which implicitly defines domain Ω in the sense that (2) holds and that we suppose continuous over $\mathbb{R}^d$, then to regularize it thanks to (3), considering the exact solution u, provided by formula (4), for the resulting Cauchy problem. For the sequel, it will prove convenient to assume moreover that the initial function u_0 is an *overestimation* of the signed distance function u_Ω to Ω, except on a tubular neighbourhood U of $\partial\Omega$, where it is exactly u_Ω, that is:

$$\forall x \in U, u_0(x) = u_\Omega(x); \quad \forall x \in \mathbb{R}^d \setminus U, |u_0(x)| \geq |u_\Omega(x)|. \tag{5}$$

We then have the following small result:

Lemma 1 *Assume Ω is a bounded open set, with smooth boundary $\partial\Omega$. For any small enough time step $dt > 0$, denote $t^n = ndt$, $n \in \mathbb{N}$. Suppose the initial function u_0 satisfies* (5) *and denote u the solution of* (3) *provided by Theorem* 2. *Then*

$$\begin{aligned}
&\forall x \in \mathbb{R}^d \setminus \Omega \quad u(t^{n+1}, x) = \inf_{\|z\| \leq dt} \big(u(t^n, x+z) + dt\big),\\
&\forall x \in \Omega \quad u(t^{n+1}, x) = \sup_{\|z\| \leq dt} \big(u(t^n, x+z) - dt\big).
\end{aligned} \tag{6}$$

Proof First, thanks to the exact formula (4), it is clear that assumption (5) on u_0 implies that for all $t > 0$ and $x \in \mathbb{R}^d$

$$|u(t,x)| \geq |u_\Omega(x)|. \tag{7}$$

By symmetry, we restrict ourselves to showing the lemma in the case $x \in \mathbb{R}^d \setminus \Omega$.

Assume first that $t^{n+1} < d(x, \partial\Omega)$. Then,

$$\begin{aligned}
u(t^{n+1}, x) &= \inf_{\|y\| \leq t^{n+1}} \Big(u_0(x+y) + t^{n+1}\Big)\\
&= \inf_{\|y\| \leq t^n,\, \|z\| \leq dt} \big(u_0(x+y+z) + t^n + dt\big)\\
&= \inf_{\|z\| \leq dt} \big(u(t^n, x+z) + dt\big),
\end{aligned}$$

the last equality holding because $d(x, \partial\Omega) > t^{n+1}$ implies that for all $\|z\| \leq dt$, $d(x+z, \partial\Omega) > t^n$.

Suppose now that $t^{n+1} \geq d(x, \partial\Omega)$, and suppose dt is smaller than the half-width of the tubular neigbourhood U of $\partial\Omega$ (on which u_Ω is assumed to be smooth, according to Theorem 1). We then have:

$$\begin{aligned}
\inf_{\|z\| \leq dt} \big(u(t^n, x+z) + dt\big) &\geq \inf_{\|z\| \leq dt} (u_\Omega(x+z) + dt)\\
&= u_\Omega(x)\\
&= u(t^{n+1}, x).
\end{aligned}$$

Conversely, either $\|x\| \leq dt$, then there exists $\|z_0\| \leq dt$ such that $(x+z_0) \in U \cap \overline{\Omega}$ and

$$\inf_{\|z\|\leq dt} \big(u(t^n, x+z) + dt\big) = u(t^n, x+z_0) + dt = u_{\Omega}(x)$$

and the result follows thanks to the above arguments, or we can choose $\|z_0\| \leq dt$ so that

$$\inf_{\|z\|\leq dt} (d(x+z, \partial\Omega)) = d(x+z_0, \partial\Omega) = d(x, \partial\Omega) - dt$$

and given that $d(x+z_0, \partial\Omega) \leq t^n$, we get eventually

$$\begin{aligned}\inf_{\|z\|\leq dt} \big(u(t^n, x+z) + dt\big) &\leq u(t^n, x+z_0) + dt \\ &= d(x+z_0, \partial\Omega) + dt \\ &= u_{\Omega}(x) \\ &= u(t^{n+1}, x),\end{aligned}$$

which concludes the proof. □

Suppose our computation is restricted to a bounded domain $\mathcal{D}$ enclosing Ω. We aim at computing function $u(t^N, .)$ over $\mathcal{D}$ for N big enough so that $t^N \geq \sup_{x\in\mathcal{D}} |u_{\Omega}(x)|$. To this end, we use the iterative formulae provided by the previous lemma, transforming them a bit so as to get a decreasing sequence of functions, using the overestimation inequality (7): introduce, for $n = 0, 1, \dots$, the sequence $\widetilde{u^n}$ of continuous functions over $\mathcal{D}$, iteratively defined by $\widetilde{u^0} = u_0$, and

$$\forall x \in \mathcal{D} \setminus \Omega, \widetilde{u^{n+1}}(x) = \inf\big(u(t^{n+1}, x), \widetilde{u^n}(x)\big), \tag{8}$$

$$\forall x \in \Omega, \widetilde{u^{n+1}}(x) = \sup\big(u(t^{n+1}, x), \widetilde{u^n}(x)\big). \tag{9}$$

From the above arguments, it follows that $\widetilde{u^n}$ is a sequence of continuous functions over $\mathcal{D}$ which converges pointwise to u_{Ω}. Furthermore, from its definition, it is clear that for $x \in \mathcal{D} \setminus \Omega$, $\widetilde{u^n}(x)$ *decreases* from $u_0(x)$ to $u_{\Omega}(x)$ and that for $x \in \Omega$, $\widetilde{u^n}(x)$ *increases* from $u_0(x)$ to $u_{\Omega}(x)$. This sequence of functions—computed thanks to the iterative process expressed in lemma 1—is the one we will try and approximate in the next section so as to end up with the desired signed distance function.

4 A numerical scheme for the signed distance function approximation

In this section, we propose a method for computing the signed distance function. The algorithm consists of two steps; the first one is purely geometric and amounts to identifying the simplices of the background mesh which intersect contour $\partial\Omega$, and the second one is purely analytical and is based on an explicit numerical scheme for solving the unsteady Eikonal equation (3).

Algorithm 1 Extending the signed distance function field

```
1: Initialize the signed distance function $u^0$ with:
     $\begin{cases} u^0(x) = \textit{exact signed distance function to } \Omega \textit{ if } x \textit{ belongs to a simplex of } \mathcal{K} \\ u^0(x) = u_{MAX} \textit{ otherwise} \end{cases}$
2: for $n = 1, \dots$ until convergence do
3:    $u^n(x) = u^{n-1}(x)$ for each node $x$ of $\mathcal{T}$
4:    for each simplex $T$ of $\mathcal{T}$ do
5:       for each node $x$ of $T$ which does not belong to a simplex in $\mathcal{K}$ do
6:          if $x \notin \Omega$ then
7:             $u^n(x) = \min\left(u^n(x), u^{n-1}\left(x - \frac{\nabla(u^{n-1}|_T)}{\|\nabla(u^{n-1}|_T)\|}dt\right)\right) + dt \quad (10)$
8:          else
9:             $u^n(x) = \max\left(u^n(x), u^{n-1}\left(x + \frac{\nabla(u^{n-1}|_T)}{\|\nabla(u^{n-1}|_T)\|}dt\right)\right) - dt \quad (11)$
10:         end if
11:      end for
12:   end for
13: end for
14: return $u^n$
```

4.1 Extending the signed distance function from the boundary

Given a polyhedral domain Ω, known by means of a simplicial mesh $\mathcal{S}$ of its boundary $\partial\Omega$, we intend to compute the signed distance function to Ω at every node x of a simplicial mesh $\mathcal{T}$ of a bounding box $\mathcal{D}$. More accurately, call $\mathcal{K} := \{K \in \mathcal{T};\ K \cap \partial\Omega \neq \emptyset\}$ the set of the simplices of $\mathcal{T}$ which intersect the boundary $\partial\Omega$. We suppose that the signed distance function is initialized to its exact value in the nodes of those simplices $K \in \mathcal{K}$, and to a great value in the other nodes so that the initialization of the algorithm satisfies (5), at least in a discrete way; see Sect. 4.2 for the implementation of this initialization. We then expect to devise an iterative numerical scheme on basis of formulae (6) to extend this signed distance function to the whole bounding domain.

To achieve this, we propose to approximate u_Ω by means of a $\mathbb{P}^1$ finite element function on mesh $\mathcal{T}$. Let dt be a time-step, $t^n = ndt$ $(n = 0, \dots)$ and u^n be a $\mathbb{P}^1$ function intended as an approximation of the unique viscosity solution u of (3) at time t^n. We then iteratively compute u^n thanks to Algorithm 1.

This algorithm needs some clarifying comments: for each step $t^n \to t^{n+1}$, we intend to mimic formulae (6), except that the infimum and supremum appearing there are difficult to compute in a discrete way. Assuming time step dt to be small enough, given for example a node of $\mathcal{T}$, $x \in \mathcal{D} \setminus \Omega$ and $n \geq 0$ the simplest approximation of $\inf_{\|z\| \leq dt} (u^n(x + z) + dt)$ is achieved considering the gradient of u^n at x. However, this gradient is a constant-per-simplex vector, and is obviously discontinuous at the interface between two adjacent simplices of $\mathcal{T}$. In particular, it is irrelevant to talk

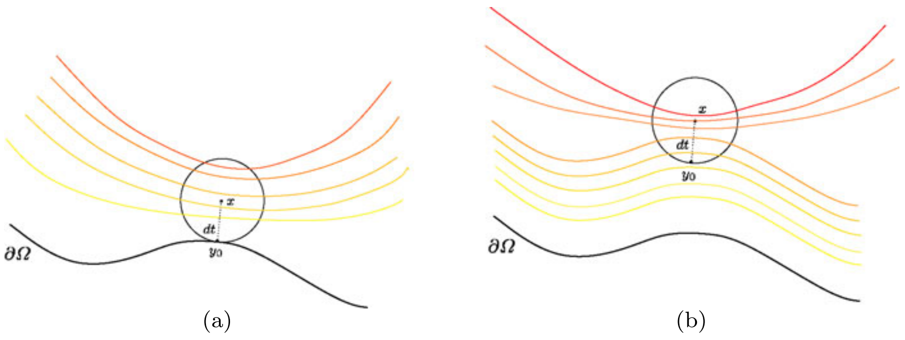

Fig. 1 At a given iteration n, the proposed numerical scheme amounts to 'regularize' the value of u^n at point x from its value at point y_0 such that $u^n(y_0) = \inf_{y \in B(x,dt)} u^n(y)$ with the property of unitary gradient, (**a**) e.g. for a point x at distance dt from $\partial\Omega$, $u^1(x) = u_0(y_0) + dt = dt = d(x, \partial\Omega)$. (**b**) The property of unit gradient 'propagates' from the boundary $\partial\Omega$, near which values of u^n are 'regularized' at an early stage

about its value at a node x of $\mathcal{T}$. The most natural way to discretize formula (6) is then

$$\inf_{\|z\| \leq dt} \left(u^n(x+z) + dt \right) \approx \inf_{T \in Ball(x)} u^n \left(x - \frac{\nabla(u^{n-1}|_T)}{\|\nabla(u^{n-1}|_T)\|} dt \right) + dt \tag{12}$$

where $Ball(x)$ is the set of simplices of mesh $\mathcal{T}$ containing x as vertex.

The rest of Algorithm 1 is merely a discrete version of formulae (8) and (9). See Fig. 1 for a visual intuition of the process.

Remark 1 Actually, a formal study of the characteristic curves of (1) and (3) would have brought more or less the same numerical scheme. In that scope, the points $x \in \mathcal{D}$ where u_Ω fails to be smooth can be interpreted as the crossing points of different characteristic curves of Eikonal equation (1); see Fig. 2. At nodes x of mesh $\mathcal{T}$ close to such kinks of the signed distance function, the discretization (12) expresses the idea that each one of these crossing characteristic curve is backtracked.

4.2 Initialization of the signed distance function near $\partial\Omega$

Before extending the signed distance function field from the boundary $\partial\Omega$, we need first to detect those simplices $K \in \mathcal{T}$ which intersect $\partial\Omega$. This is achieved by scanning each surface triangle $T \in \mathcal{S}$ in three dimensions (segment in two dimensions), storing a background mesh simplex $K \in \mathcal{T}$ containing one of the three nodes of T, then travelling the background mesh from K by adjacency, advancing only through faces which intersect T. Figure 3 illustrates this step. A computationally efficient algorithm for the three-dimensional triangle-triangle overlap test, relying only on predicates, developed in [21] is used to this end.

Then, at each node of K which belongs to such an intersecting simplex, we initialize the (still unsigned) distance function to its exact value. See [25] for an efficient

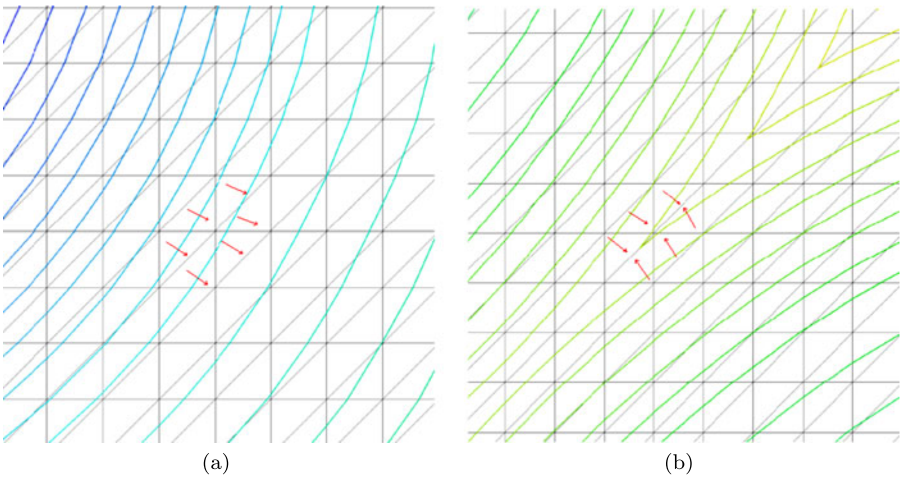
Fig. 2 (**a**) Continuity of the gradient in the areas where the signed distance function is regular; (**b**) discontinuity of the gradient at a node close to the skeleton

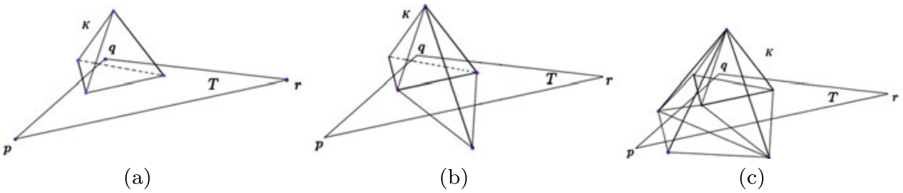

Fig. 3 Recovery of the background simplices intersecting a triangle $T = (pqr) \in \mathcal{S}$: (**a**) one starts with a simplex K of $\mathcal{T}$ containing one of the points p, q or r then (**b**) marches through the faces of K which intersect T and (**c**) goes on, stopping when there is no more simplex of K to add

algorithm computing a point-triangle distance in three dimensions. In all the other nodes of $\mathcal{T}$, we assign an arbitrary large value (e.g. larger than the domain size).

This leaves us with initializing the sign. Surprisingly enough, this stage happens to be the most tedious one of the initialization process, all the more so as it is barely considered in the literature (see nevertheless [39] for another approach, based on an octree grid refinement). We propose here a purely logical Algorithm 2 based on a progression by "layers", which relies on two piles *Layer* and *Boundary*, and an integer *Sign*. It is very similar to the classical coloring techniques used to recover the connected components of a configuration in a Delaunay meshing context [17]; see Fig. 4.

So as to enhance the numerical efficiency of the proposed method, several improvements have been proposed to this algorithm. Note that the propagating scheme (1) is inherently parallel: at a given step, the operations carried out in a background simplex K are independent from those carried out in another such simplex. Furthermore, the time step dt must be chosen small enough at the beginning of the process, so that going back along the characteristic lines does not lead to crossing the interface $\partial\Omega$ and picking irrelevant values. But after a certain amount of iterations, we can ob-

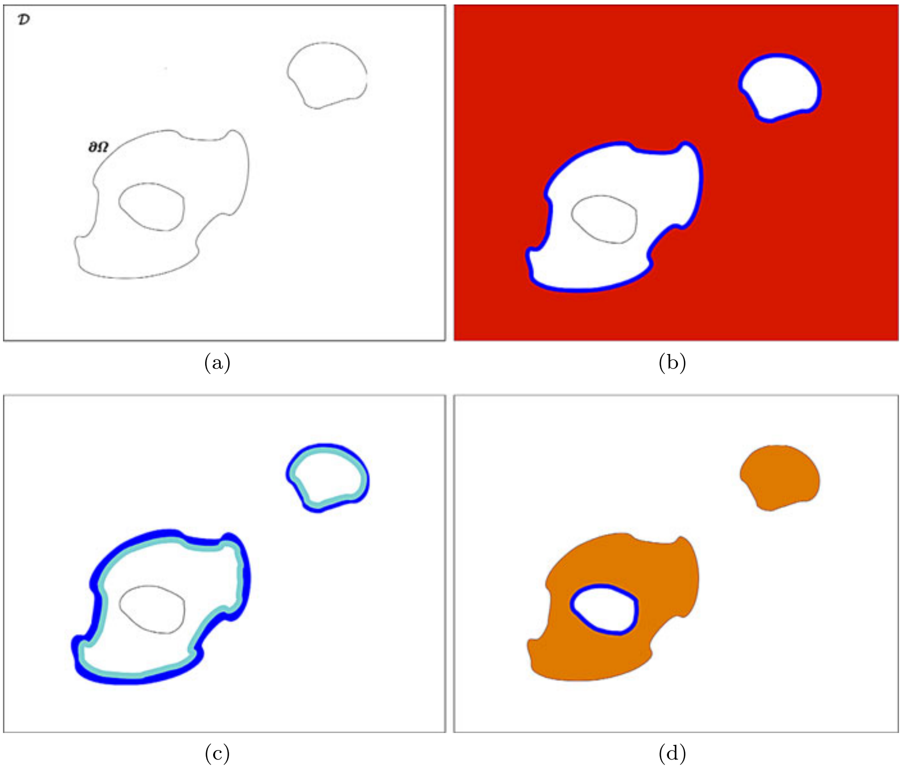

Fig. 4 (Color online) Signing the unsigned initial distance field; (**a**) A contour $\partial\Omega$, (**b**) start from a triangle of the computational mesh $\mathcal{T}$ that is known to be in the exterior to the domain Ω, travel $\mathcal{T}$ by adjacency and recover the first (outer) layer (*in red*), and the simplices of $\mathcal{T}$ intersecting the part of $\partial\Omega$ connected to this first layer (*in blue*) (**c**) Get all the triangles of $\mathcal{T}$ (*in pale blue*) that are the different starting points for the new (now interior) layer, (**d**) travel again by adjacency to get this new layer (*in orange*), as well as the new simplices of $\mathcal{T}$ intersecting the part of $\partial\Omega$ connected to this layer (*in blue*)

viously increase this time step. Eventually, note that Theorem 2 expresses the fact that the information propagates from $\partial\Omega$ to the whole space with a unitary velocity—that is to say that, on the theoretical framework, at a given point $x \in \mathbb{R}^d$, $u(s, x) = u_\Omega(x)$ for all time $s > d(x, \partial\Omega)$. According to this observation, we decided to fix the values computed at a node x when these values are smaller than the current total time of the propagation (with a security margin).

5 Mesh adaptation for a sharper approximation of the signed distance function

We approximate the signed distance function to Ω by means of a $\mathbb{P}^1$ finite elements function; therefore it seems natural to attempt to decrease the interpolation error of this function on the background mesh $\mathcal{T}$. Moreover, if we intend to use the signed distance function to Ω as the initial implicit function defining Ω when using level set methods, we may want the 0 level set of the approximated signed distance function

Algorithm 2 Signing the unsigned initial distance field

```
1:  Initialize pile Layer with a simplex $K \in \mathcal{T}$ which is in the "most external" connected component of the configuration (for instance a simplex in the corner of the bounding box).
    Initialize Sign to $+1$.
2:  while an element $K$ in pile Layer as not been inspected do
3:      Consider every neighbour $K'$ of $K$: if $K'$ has not yet been inspected, and does not belong to $\mathcal{K}$, put $K'$ in Layer; if $K'$ belongs to $\mathcal{K}$, put it into pile Boundary.
4:  end while
5:  while an element $K$ in Boundary has not yet been inspected do
6:      Consider every neighbour $K'$ of $K$: if $K'$ has not yet been inspected, and belongs to $\mathcal{K}$, put $K'$ in pile Boundary (this step ensures pile Boundary contains all the boundary elements corresponding to the ongoing layer).
7:  end while
8:  Put the current sign of Sgn in each vertex of each element of pile Stratum.
9:  $Sign \leftarrow -Sign$.
10: Clean pile Layer.
11: for $K$ is in pile Boundary do
12:     Consider every neighbour $K'$ of $K$: if $K'$ has not yet been inspected, put it into pile Layer: then we get all the new starting points of the new layer (possibly associated to different connected components of $\Omega$.
13: end for
14: Clean pile Boundary.
15: Go back to step 2.
```

(which is intended to be close to the $\mathbb{P}^1$ interpolant of this function) to match as much as possible the true boundary $\partial\Omega$. Thus it can be interesting to couple the computation of the signed distance function with a process of adaptation of the background mesh $\mathcal{T}$. Actually, we will see that adapting $\mathcal{T}$ the same way leads to an improvement as regards both problems.

5.1 Anisotropic mesh adaptation

Mesh adaptation basically lies on the fact that the most efficient way to refine a mesh so as to increase the efficiency of computations is to adjust the directions and sizes of its elements in agreement with the variations of the functions under consideration. Thus, significant improvements can be achieved in accuracy, while the cost of the computations (related to the total number of elements of the mesh) is kept minimal, and conversely.

Numerous methods exist as regards the very popular topic of mesh adaptation, some of them relying on the concepts of Riemannian metric [22]: the local desired size, shape and orientation related information at a node x of mesh $\mathcal{T}$ is stored in a metric tensor field $M(x)$, prescribed by an error indicator or an error estimate which can arise from various possible preoccupations: a posteriori geometric error estimates, analytic error estimates, etc.... (see for instance [2, 4, 23]).

Given a metric tensor field $M(x)$ defined at each point $x \in \mathbb{R}^d$, (notice that in practice, $M(x)$ is defined only at the nodes of $\mathcal{T}$ and then interpolated from these values [17]) we consider respectively the *length* $l_M(\gamma)$ of a curve $\gamma : [0,1] \to \mathbb{R}^d$ and the *volume* $V_M(K)$ of a simplex K in the Riemannian space $(\mathbb{R}^d, M)$:

$$l_M(\gamma) = \int_0^1 \sqrt{\langle M(\gamma(t))\gamma'(t), \gamma'(t)\rangle} dt, \quad V_M(K) = \int_K \sqrt{\det(M(x))} dx$$

and aim at modifying the mesh $\mathcal{T}$ so as to make it *quasi-unit* with respect to the metric $M(x)$, that is to say all its simplices K have edges lengths lying in $[\frac{1}{\sqrt{2}}, \sqrt{2}]$ and an *anisotropic quality measure*:

$$\mathcal{Q}_M(K) := \alpha_d \frac{V_M(K)^2}{(\sum_{i=1}^{na} l_M(e_i)^2)^d}$$

close to 1 (where $na = d(d+1)/2$ is the number of edges of a d-dimensional simplex, e_i are the edges of K and α_d is a normalization factor). For instance, in the particular case when $M(x)$ is constant over $\mathbb{R}^d$, M can be characterized by the ellipsoid

$$\Phi_M(1) = \left\{ v \in \mathbb{R}^d / \, l_M(v) = 1 \right\}$$

of unit vectors with respect to M, and a simplex K with unit edges is simply a simplex enclosed in this ellipsoid.

Several techniques have been devised for generating anisotropic meshes according to a metric tensor field, that can be roughly classified into two categories. On the one hand, global methods, such as Delaunay-based methods and advancing-front methods, perform the same kind of operations as in the classical case with adapted notions of length and volume. On the other hand, local mesh modification methods [18] start from an existing non-adapted mesh and adapt it so that it fits at best the above conditions. The approach used in this paper belongs to the second category.

5.2 Computation of a metric tensor associated to the minimization of the $\mathbb{P}^1$ interpolation error

Let us recall the following result (whose proof lies in [3, 13]) about the interpolation error of a smooth function u on a simplicial mesh by means of a $\mathbb{P}^1$ finite elements function, in L^∞ norm.

Theorem 3 *Let $\mathcal{T}$ a simplicial mesh of a polyhedral domain $\mathcal{D} \subset \mathbb{R}^d$ ($d = 2$ or 3) and u a $\mathcal{C}^2$ function on $\mathcal{D}$. Let $V_\mathcal{T}$ the space of continuous functions on $\mathcal{D}$ whose restriction to every simplex of $\mathcal{T}$ is a $\mathbb{P}^1$ function, and denote by $\pi_\mathcal{T} : \mathcal{C}(\mathcal{D}) \to V_\mathcal{T}$ the usual $\mathbb{P}^1$ finite elements interpolation operator. Then for every simplex $K \in \mathcal{T}$,*

$$\|u - \pi_\mathcal{T} u\|_{L^\infty(K)} \leq \frac{1}{2}\left(\frac{d}{d+1}\right)^2 \max_{x \in K} \max_{y,z \in K} \langle |\mathcal{H}(u)|(x) yz, yz \rangle$$

where, for a symmetric matrix $S \in \mathcal{S}_d(\mathbb{R})$, which admits the following diagonal shape in orthonormal basis

$$S = P \begin{pmatrix} \lambda_1 & 0 & \cdots & 0 \\ \vdots & \vdots & \ddots & \vdots \\ 0 & \cdots & 0 & \lambda_d \end{pmatrix} {}^t P,$$

we denote

$$|S| := P \begin{pmatrix} |\lambda_1| & 0 & \cdots & 0 \\ \vdots & \vdots & \ddots & \vdots \\ 0 & \cdots & 0 & |\lambda_d| \end{pmatrix} {}^t P.$$

Relying on this theorem, we build a metric tensor field $M(x)$ on $\mathcal{D}$ that allows an accurate control of the L^∞ interpolation error of u (recall the main feature of this interpolation error is that it is an upper bound for the approximation error of u by means of a finite elements calculus with the space $V_{\mathcal{T}}$, at least in the case of elliptic problems [10]): so as to get

$$\forall K \in \mathcal{T}, \quad \|u - \pi_{\mathcal{T}} u\|_{L^\infty(K)} \le \epsilon$$

for a prescribed margin $\epsilon > 0$. We urge the shape of an element K of $\mathcal{T}$ to behave in such a way that

$$\max_{y,z \in K} \langle \widetilde{\mathcal{H}} yz, yz \rangle \le c\epsilon$$

where c is a constant which only depends on the dimension, stemming from Theorem 3 and $\widetilde{\mathcal{H}}$ is the mean value (or an approximation) of the metric tensor $|\mathcal{H}(u)|$ over element K. This leads to defining the desired metric tensor $M(x)$ at each node x of $\mathcal{T}$ by (see [1, 2]):

$$M(x) = P(x) \begin{pmatrix} \widetilde{\lambda_1} & 0 & 0 \\ 0 & \widetilde{\lambda_2} & 0 \\ 0 & 0 & \widetilde{\lambda_3} \end{pmatrix} {}^t P(x) \tag{13}$$

where

$$\widetilde{\lambda_i} = \min\left(\max\left(\frac{c|\lambda_i|}{\epsilon}, \frac{1}{{h_{max}}^2} \right), \frac{1}{{h_{min}}^2} \right),$$

$$\widetilde{|\mathcal{H}(u)|}(x) = P(x) \begin{pmatrix} |\lambda_1| & 0 & 0 \\ 0 & |\lambda_2| & 0 \\ 0 & 0 & |\lambda_3| \end{pmatrix} {}^t P(x)$$

being an approximation of the Hessian of u around node x, written here in diagonal form in an orthonormal basis, h_{min} (resp. h_{max}) being the smallest (resp. largest) size allowed for an element in any direction, and c being the above constant.

5.3 Mesh adaptation for a geometric reconstruction of the 0 level set of a function

In this section, we consider a bounded domain $\Omega \subset \mathbb{R}^d$, implicitly defined by a function u—that is, $\Omega = \{x \in \mathbb{R}^d / u(x) < 0\}$ and $\partial\Omega = \{x \in \mathbb{R}^d / u(x) = 0\}$—and we want to adapt the background mesh $\mathcal{T}$ so that the 0-level set of the function $\pi_{\mathcal{T}} u_\Omega$ obtained from u by $\mathbb{P}^1$ finite elements interpolation, say $\partial\Omega_{\mathcal{T}}$, is as close as possible to the 0-level set of the true function u, in terms of the Hausdorff distance (for a review of the various methods for discretizing an implicit surface, see [20]). Then we will apply these results to the particular case when u is the signed distance function to Ω. Throughout this section, we follow the previous work in [15].

Definition 3 Let K_1, K_2 two compact subsets of $\mathbb{R}^d$. For all $x \in \mathbb{R}^d$, denote $d(x, K_1) = \inf_{y \in K_1} d(x, y)$ the *Euclidean distance from x to K_1*. We define:

$$\rho(K_1, K_2) := \sup_{x \in K_1} d(x, K_2)$$

and call *Hausdorff distance between K_1 and K_2*, denoted by $d^H(K_1, K_2)$, the non-negative real number

$$d^H(K_1, K_2) := \max(\rho(K_1, K_2), \rho(K_2, K_1)).$$

The following small lemma will come in handy when we have to measure the distance to Ω thanks to u:

Lemma 2 *Let u a $\mathcal{C}^1$ function on a tubular neighbourhood W of $\partial\Omega$, without any critical point on W, so that the set $\partial\Omega$ is a submanifold of $\mathbb{R}^d$, and Ω is a bounded subdomain of $\mathbb{R}^d$ with $\mathcal{C}^1$ boundary. For any point $x \in W$ we have the estimate*:

$$d(x, \partial\Omega) \leq \frac{\sup_{z \in \mathbb{R}^d} \|\nabla u(z)\|}{\inf_{z \in \mathbb{R}^d} \|\nabla u(z)\|^2} |u(x)|. \tag{14}$$

Proof The proof consists in 'going backwards' following the velocity field ∇u until going against $\partial\Omega$, then to estimate the distance between x and the contact point with $\partial\Omega$. To achieve this, introduce the characteristic curve γ associated to the field ∇u and starting from x, defined as a solution of the EDO:

$$\begin{cases} \gamma(0) = x \\ \gamma'(s) = \nabla u(\gamma(s)). \end{cases} \tag{15}$$

Owing to classical arguments concerning ODE, the curve $s \mapsto \gamma(s)$ is defined for all real values s—including negative ones—and there exists a real number s_0, positive or negative if, respectively $x \in \Omega$ or $x \in {}^c\Omega$, such that $y := \gamma(s_0)$ belongs to $\partial\Omega$, because u has no critical point on W. We then have:

$$\begin{aligned} u(x) &= u(x) - u(y) \\ &= \int_{s_0}^{0} \langle \nabla u(\gamma(s)), \gamma'(s) ds \rangle \\ &= \int_{s_0}^{0} \|\nabla u(\gamma(s))\|^2 ds \end{aligned}$$

and thus obtain

$$|s_0| \inf_{z \in \mathbb{R}^d} \|\nabla u(z)\|^2 \leq |u(x)|. \tag{16}$$

On the other hand, we also get

$$x - y = \int_{s_0}^{0} \nabla u(\gamma(s)) ds$$

and

$$\|x - y\| \leq |s_0| \sup_{z \in \mathbb{R}^d} \|\nabla u(z)\|. \tag{17}$$

Note that, in practice, the computational domain $\mathbb{R}^d$ is restricted to a bounding box containing Ω, so that taking supremum or infimum in this framework does not pose any problem. Eventually, with (16) and (17), we conclude that:

$$d(x,\partial\Omega) \leq \|x-y\| \leq \frac{\sup_{z\in\mathbb{R}^d}\|\nabla u(z)\|}{\inf_{z\in\mathbb{R}^d}\|\nabla u(z)\|^2}|u(x)|. \qquad \square$$

Note that formula (15) expresses the idea that the closer u is to the signed distance function to Ω (or a fixed multiple of it), the more we can rely on the evaluation of u to estimate the Euclidean distance to the boundary $\partial\Omega$.

We are now ready to estimate the Hausdorff distance between $\partial\Omega$ and $\partial\Omega_{\mathcal{T}}$. Take a point $x\in\partial\Omega_{\mathcal{T}}$, which belongs to a simplex K of the background mesh $\mathcal{T}$. With Lemma 2 we have

$$\begin{aligned} d(x,\partial\Omega) &\leq \frac{\sup_{y\in\mathbb{R}^d}\|\nabla u(y)\|}{\inf_{y\in\mathbb{R}^d}\|\nabla u(y)\|^2}|u(x)| \\ &= \frac{\sup_{y\in\mathbb{R}^d}\|\nabla u(y)\|}{\inf_{y\in\mathbb{R}^d}\|\nabla u(y)\|^2}|u(x)-\pi_{\mathcal{T}}u(x)| \end{aligned}$$

and it yields, thanks to Theorem 3

$$d(x,\partial\Omega) \leq c\frac{\sup_{y\in\mathbb{R}^d}\|\nabla u(y)\|}{\inf_{y\in\mathbb{R}^d}\|\nabla u(y)\|^2}\max_{x\in K}\max_{y,z\in K}\langle|\mathcal{H}(u)|(x)yz, yz\rangle$$

where c is a scalar constant which only depends on d. Thus, we find

$$\rho(\partial\Omega_{\mathcal{T}},\partial\Omega) \leq c\frac{\sup_{y\in\mathbb{R}^d}\|\nabla u(y)\|}{\inf_{y\in\mathbb{R}^d}\|\nabla u(y)\|^2}\max_{K\in\mathcal{T}}\max_{x\in K}\max_{y,z\in K}\langle|\mathcal{H}(u)|(x)yz, yz\rangle.$$

By the same token, applied to a point $x\in\partial\Omega$, we have

$$\rho(\partial\Omega,\partial\Omega_{\mathcal{T}}) \leq c\frac{\sup_{K\in\mathcal{T}}\|\nabla u_{\mathcal{T}}|_K\|}{\inf_{K\in\mathcal{T}}\|\nabla u_{\mathcal{T}}|_K\|^2}\max_{K\in\mathcal{T}}\max_{x\in K}\max_{y,z\in K}\langle|\mathcal{H}(u)|(x)yz, yz\rangle.$$

Eventually, neglecting the discrepancy between $\|\nabla u\|$ and $\|\nabla u_{\mathcal{T}}\|$ yields:

$$d^H(\partial\Omega,\partial\Omega_{\mathcal{T}}) \leq c\frac{\sup_{y\in\mathbb{R}^d}\|\nabla u(y)\|}{\inf_{y\in\mathbb{R}^d}\|\nabla u(y)\|^2}\max_{K\in\mathcal{T}}\max_{x\in K}\max_{y,z\in K}\langle|\mathcal{H}(u)|(x)yz, yz\rangle.$$

We observe that this estimate is very similar to the result given by Theorem 3, and especially that it involves the Hessian matrix of u; thus, with the same metric tensor field (13) as the one associated to the control of the $\mathbb{P}^1$-interpolation error on $\mathcal{T}$, we achieve control of the Hausdorff distance between the exact boundary $\partial\Omega$ and its piecewise affine reconstruction $\partial\Omega_{\mathcal{T}}$. Of course, depending on where we need the accuracy, we can restrict ourselves to prescribing metric (13) only in certain areas of $\mathbb{R}^d$ (e.g. in a level set context, in a narrow band near the boundary, or in the vicinity of a particular isosurface of u).

This result admits a rather interesting geometric interpretation in the case when $u=u_\Omega$, i.e. when u is a signed distance function. In that case, it is well-known [6] the second fundamental form reads, for any point $x\in\partial\Omega$:

$$\forall\xi\in T_x\partial\Omega, \quad \mathbf{II}_x(\xi,\xi) = -\langle\mathcal{H}u(x)\xi,\xi\rangle$$

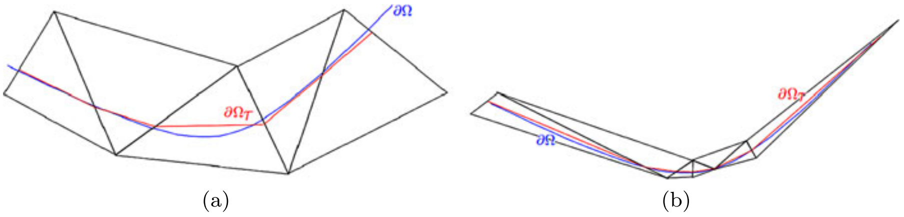

Fig. 5 $\mathbb{P}^1$-reconstruction of $\partial\Omega$ with (**a**) a regular background mesh $\mathcal{T}$ and (**b**) an adapted anisotropic background mesh $\mathcal{T}$

where $\langle ., . \rangle$ denotes the usual Euclidean scalar product of $\mathbb{R}^d$. Hence, up to the sign, the eigenvalues of $\mathcal{H}u(x)$ are the two principal curvatures of the surface $\partial\Omega$, associated with the two principal directions at point x. In such case, the above estimates mean that, understandingly enough, so as to get the best reconstruction of $\partial\Omega$, we have to align the circumscribed ellipsoids of the simplices of the background mesh $\mathcal{T}$ with the curvature of this surface (see Fig. 5).

6 A remark about level-set redistancing

When evolving an interface by means of the level set method—e.g. when dealing with multi-phase flow systems—a crucial issue is to maintain the level set function $\phi^n = \phi(t^n, .)$ ($t^n = ndt$, where dt is the time step of the process) as close as possible to the signed distance function to the zero level set $\partial\Omega^n$ so defined, while it tends to get very far from it in few iteration steps (see e.g. [28] for the relevance of this feature in the context of multi-phase flows). To achieve this, a redistancing step must be carried out [9]. Unfortunately, it is worth emphasizing this problem is ill-posed since it is impossible to "regularize" function ϕ^n to make it close to a distance function $\widetilde{\phi^n}$—i.e. $\|\nabla\widetilde{\phi^n}\| \approx 1$—without changing the zero level-set which then becomes $\widetilde{\partial\Omega^n} := \{x \in \mathbb{R}^d / \widetilde{\phi^n}(x) = 0\}$. Several approaches exist to address this issue, depending on the applications they are suited for and thus on the features of the interface $\partial\Omega^n$ which must be retained (see e.g. [29, 32, 40, 41]).

Given an iteration n when this process is to be carried out, most of these approaches consist in solving the *unsteady Eikonal equation* (3), with initial data ϕ^n and over a short time period, so that the obtained solution enjoys the unitary gradient property, at least in a neighborhood of the tracked interface. To this end, in [8, 38, 40], an approximation of the sign function that appears in (3) by a smooth, steep function is introduced. The overall process is very fast, since the only performed operations are a few iterations of an often explicit scheme for (3). In particular, this trick of approximating the sign function enables not to regenerate an exact distance function near the boundary as we explained in Sect. 4.2, which can be costly if the computational mesh is big (see Sect. 8). The drawback is that the shift in the considered interface is not controlled.

Hence, we limit ourselves to the case of an adaptation process, where at each step, the background mesh $\mathcal{T}$ is adapted to the zero level-set of function ϕ^n, by prescribing the metric tensor field (13) at least in a narrow band near the interface (see [7] for an example). Here, implementing the redistancing step $\phi^n \to \widetilde{\phi^n}$ by taking for $\widetilde{\phi^n}$ the signed distance function to Ω^n, computed by means of the algorithm devised in Sect. 4, provides a true signed distance function $\widetilde{\phi^n}$, while ensuring the movement of the interface is controlled by:

$$d^H(\partial\Omega^n, \partial\widetilde{\Omega^n}) \leq \epsilon.$$

Of course, this process is slower than the one discussed above, but we believe it can be of interest when an close control of the change in interfaces $\partial\Omega^n \to \partial\widetilde{\Omega^n}$ is sought.

7 Extension to the computation of the signed distance function in a Riemannian space

The proposed method admits a straightforward extension in the case we want to compute the signed distance function u_Ω^M from a subdomain Ω of $\mathbb{R}^d$, *$\mathbb{R}^d$ being endowed with a Riemannian metric M*, that is,

$$u_\Omega^M(x) = \begin{cases} -d_M(x, \partial\Omega) & \text{if } x \in \Omega, \\ 0 & \text{if } x \in \partial\Omega, \\ d_M(x, \partial\Omega) & \text{if } x \in^c \overline{\Omega}, \end{cases}$$

where $d_M(x, y) = \inf_{\gamma(0)=x\,;\,\gamma(1)=y} l_M(\gamma)$ is the *distance* from x to y in the space $(\mathbb{R}^d, M)$ and $d_M(x, \partial\Omega) = \inf_{y\in\partial\Omega} d_M(x, y)$ is the *unsigned distance function from x to $\partial\Omega$*. For another approach, based on the Fast Marching Method, see [26, 34].

Indeed, the function u_Ω^M is a solution of the *Eikonal equation in the space* $(\mathbb{R}^d, M)$ in the sense of viscosity [27]:

$$\sqrt{\langle M^{-1}(x)\nabla u(x), \nabla u(x)\rangle} = 1.$$

Considering a continuous function u_0 which implicitly defines Ω in the sense that (2) holds, we have the corresponding unsteady equation:

$$\begin{cases} \dfrac{\partial u}{\partial t}(t, x) + sgn(u_0(x))(\sqrt{\langle M^{-1}(x)\nabla u(t, x), \nabla u(t, x)\rangle} - 1) = 0 \\ \hfill u(t = 0, x) = u_0(x) \end{cases}$$

and the same study as in Sect. 3 yields the following approximation formulae for computing the solution u of this equation: for $t > 0$, a small time step dt, and $x \in \overline{{}^c\Omega}$:

$$u(t + dt, x) \approx u\left(t, x - dt\frac{M^{-1}(x)\nabla u(t, x)}{\sqrt{\langle M^{-1}(x)\nabla u(t, x), \nabla u(t, x)\rangle}}\right) + dt$$

and, by symmetry, for $x \in \Omega$:

$$u(t + dt, x) \approx u\left(t, x + dt\frac{M^{-1}(x)\nabla u(t, x)}{\sqrt{\langle M^{-1}(x)\nabla u(t, x), \nabla u(t, x)\rangle}}\right) - dt$$

which raises a numerical scheme similar to the scheme presented in Sect. 4 (see Fig. 9 for an example).

Table 1 Computation of the signed distance function to the contour 6(a) on non-adapted, unstructured meshes

Number of vertices	$\|e\|_{L^\infty}$	Order	$\|e\|_{L^1}$	Order	$\|e\|_{L^2}$	Order	CPU time (s)
2601	0.013723	–	0.000924	–	0.002474	–	0.167
10201	0.008922	0.63	0.000644	0.53	0.001687	0.56	0.462
40401	0.004971	0.74	0.000340	0.73	0.000932	0.71	1.362
74310	0.001731	1.23	0.000204	0.90	0.000476	0.98	2.974
296740	0.001790	0.86	0.000095	0.96	0.000232	0.99	10.293

8 Numerical examples

Now, we provide several examples to assess the main theoretical issues presented in the previous sections. All the following computations are held on contours embedded in a bounding box which is a unit square in two dimensions, or a unit cube in three dimensions, and are scaled if need be.

Example 1 We give a 2-dimensional example of the computation of the signed distance function to the contour represented in Fig. 6, and carry out two numerical experiments.

We first hold computations on unstructured, yet non-adapted simplicial computational meshes $\mathcal{T}$ of bounding box $\mathcal{D}$, of increasing sizes, so as to assess both convergence and scaling of the method. For all these examples, a time step $dt = 0.001$ (according to the smallest mesh size among the presented meshes) is used for the steps $1 \leq n \leq 80$, and the computation is finished with a time step $dt = 0.004$. Table 1 displays several features of the computation (number of vertices of the mesh, CPU time) as well as errors measured in several norms, and an inferred approximate order for the scheme. The exact signed distance function (or more accurately its $\mathbb{P}^1$-interpolate on the mesh at stake) is computed by a brute force approach—i.e. by computing the minimum distance to a segment of the mesh of the contour at every node of the background mesh $\mathcal{T}$. All our computations are held on an OPTERON 6100, 2 GHz. Figure 6 displays the result of the computation held on the finest grid—identification of the connected components, initialization of the sign and computation of the signed distance function.

Let us make some comments at this point. We solve the *time-dependent* Eikonal equation, so that at first glance, it could be relevant to investigate both time and spatial accuracy of the proposed numerical scheme. Actually, it turns out that the spatial accuracy of the scheme is by far the most critical issue as regards convergence inasmuch as, provided time step dt is small enough (and in all the test-cases we implemented, taking dt of the order of the mesh size proved sufficient), the quality of the final result only depends on the closeness of spatial approximation.

As far as spatial convergence of this scheme is concerned, one observes that, understandably enough, it happens to be at most first-order. Is seems to behave comparably to the algorithm presented in [29] or to the simplicial version of the Fast

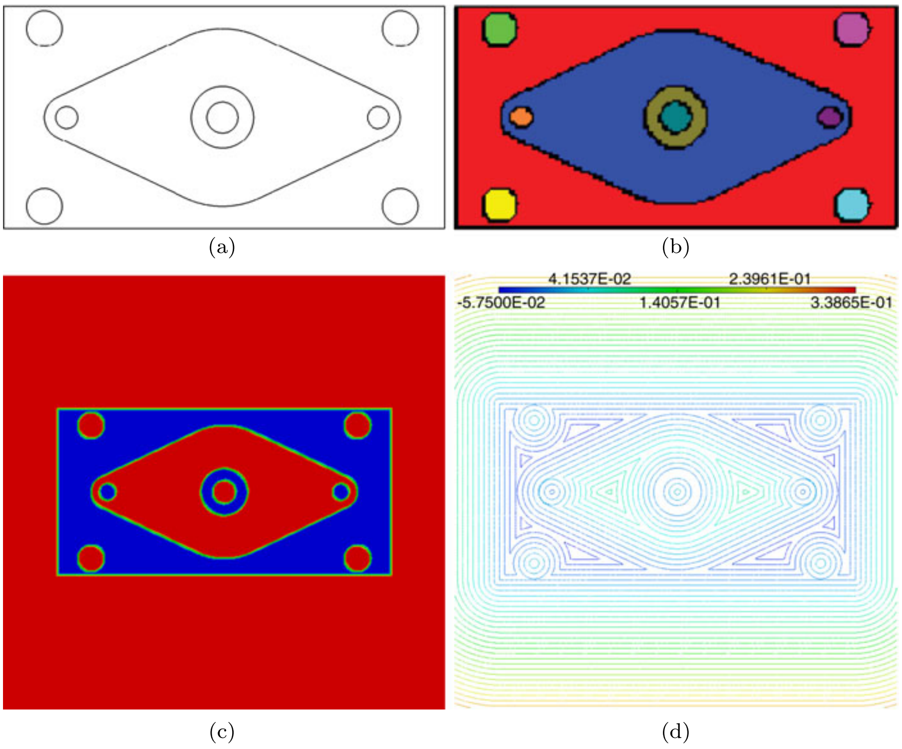

Fig. 6 (Color online) 2D example on a regular mesh; (**a**) the 2D contour, (**b**) the connected components of the contour, (**c**) sign of these components: *red* for positive, *blue* for negative, *green* for the boundary, (**d**) some isolines of the signed distance function

Marching algorithm proposed in [26] or of the Fast Sweeping algorithm, described in [31]. Note however that the two latter schemes are probably a bit faster as regards computational time, given they achieve convergence within a fixed (or very limited) number of iterations that are linear in the number of vertices of the mesh. However, we believe that differences in the architectures of the computers used to run the proposed examples are tremendous and do not allow for a meaningful comparison between the execution times of the proposed algorithms. This scheme is also bound to be slower than the ones devised in the case of Cartesian computational grids [35, 39, 40, 42], which enjoy immediate standard operation algorithms (e.g. search of the element in which a given point dwells, etc. . . .). What is more, higher-order distancing or redistancing numerical schemes are available in this Cartesian frame [8], whereas, to our knowledge, it is not this case in the unstructured case, which we believe to be of independent relevance.

Now, we adapt the background mesh $\mathcal{T}$ to the computation of the signed distance function to the same contour, relying on the principles enunciated in Sect. 5.1, in the vicinity of the boundary $\partial\Omega$. Therefore, we are only interested in getting a close approximation of this signed distance function near the boundary. We use parameters

Table 2 Computation of the signed distance function to the contour 6(a) on an adapted mesh

Number of iterations	Number of nodes	Number of elements	CPU time (seconds)
236	8,030	16,006	0.42

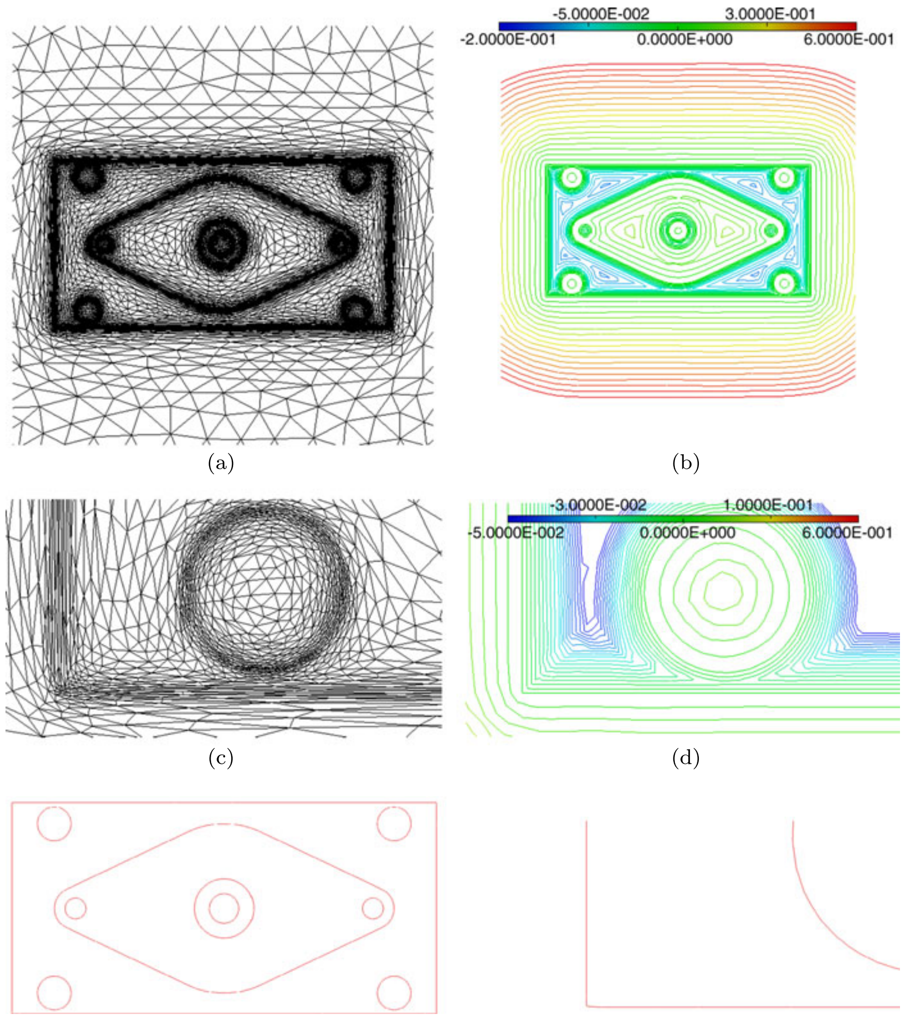

Fig. 7 2D example on an adapted mesh; (**a**) the associated adapted mesh (**b**) some isolines of the signed distance function on this mesh (**c**) a detail in the background mesh (**d**) the corresponding detail among the isolines (**e**) the piecewise affine reconstructed contour and (**f**) a zoom on a corner of the reconstructed contour

$\epsilon = 0.001$ and $h_{min} = 0.001$. This yields the results of Fig. 7, whose features (on one CPU) are reported in Table 2.

Table 3 Computation of the signed distance function to several subdomains of $\mathbb{R}^3$

	Number of faces	Number of iterations	Number of nodes	Number of elements	CPU Time (seconds)
Cimplex	4,160	227	39,593	208,676	4.13
Wheel	19,972	194	367,236	2,065,767	46.641
Happy Buddha	1,085,477	160	549,818	3,218,519	1,294
Venus (isotropic)	63,940	212	2,265,359	13,482,983	225
Venus (anisotropic)	63,940	238	120,404	670,746	605

Example 2 We now turn to the three-dimensional case. Some details about the mesh sizes and CPU times are to be found in Table 3. We tested our algorithm with the same procedure as before as regards the choice of the time step, and with a parallel implementation on 10 CPU, with a shared memory architecture. Note that only the stage corresponding to the propagation of the distance throughout the domain has been parallelized, and that the initialization step—which could also be easily parallelized—actually takes most of the computation time (Table 3 provides the number of faces of each initial contour so as to emphasize this feature). However, we thought it better to report in Table 3 the total computation time. First, we considered a mechanical part called *cimplex*. Figure 8 shows the original boundary, its reconstruction as the 0 level set of the computed approximation of the signed distance function to this contour, a level set of the computed function, and some cut in the adapted mesh. Note that the anisotropic feature of the background mesh $\mathcal{T}$ allows a good approximation of the ridges of the contour, even though we did not apply any special process to achieve so. Actually, it is worth mentioning that some post-treatment could be implemented so as to recover *exactly* those sharp features in the reconstruction of the interface $\partial\Omega$ [30], but we believe this goes beyond the scope of this paper.

The next example, hereafter named *wheel* (Fig. 10), emphasizes another difficulty that may arise, especially when it comes to mechanical devices, exhibiting very fine structures (or more generally, very fine details). They are very difficult to track accurately when the background mesh $\mathcal{T}$ is regular, the reason being the suitable size of a regular mesh for this purpose would be tremendous. Independently, note that the surface mesh of the 0 level set of the computed signed distance function reconstructed by means of intersections with the background mesh $\mathcal{T}$ may be very irregular and contain two much surface elements to allow any further calculation on it. To this end, it is often necessary to proceed to a surface remeshing step in order to generate a suitable computational mesh (see [17]). An example is provided in Fig. 10.

Then, Fig. 11 gives another example, this of the computation of the signed distance function to the Stanford *Happy Buddha*, and of the approximation of this contour as the 0 level set of the computed function.

Eventually, in several cases, for very detailed contours, we thought necessary to perform an isotropic adaptation of the background mesh, and to make an intermediate computation of the signed distance function on it before indulging in an anisotropic adaptation of the background mesh, so as to make sure to capture any close detail of the contour. See Fig. 12 and Table 3 for a comparison between both meshes.

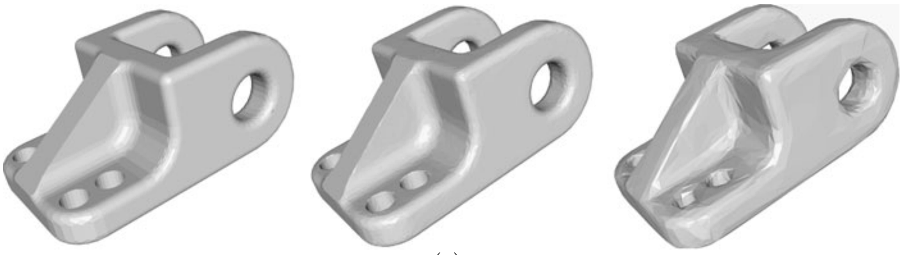
(a)

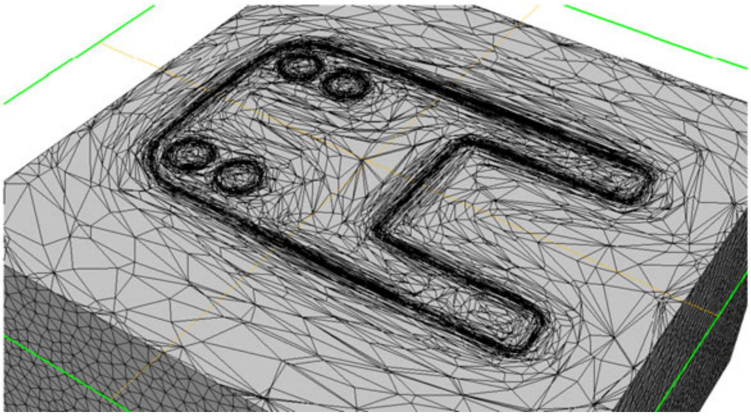
(b)

Fig. 8 Computation of the signed distance function to the 'cimplex'; (**a**) *left*—the initial domain, *center*—the reconstructed domain, *right*—isovalue 0.01 of the computed signed distance function, (**b**) A cut in the adapted mesh

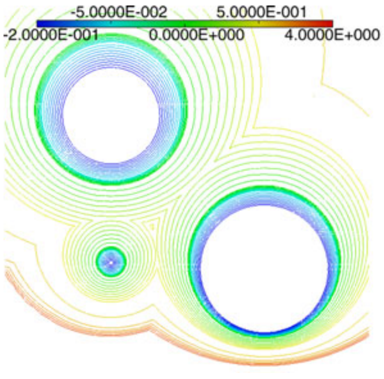

(a)

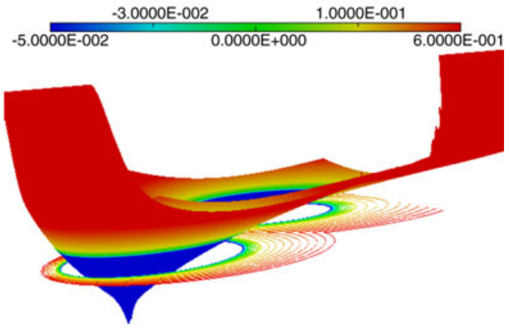

(b)

Fig. 9 (**a**) Level sets of the signed distance function to three disks embedded in the Poincaré half-plane. (**b**) 3D graph of the function

Example 3 So as to illustrate the idea hinted at in Sect. 7, our last example concerns the computation of the signed distance function to a domain $\Omega \subset \mathbb{R}^2$, $\mathbb{R}^2$ being en-

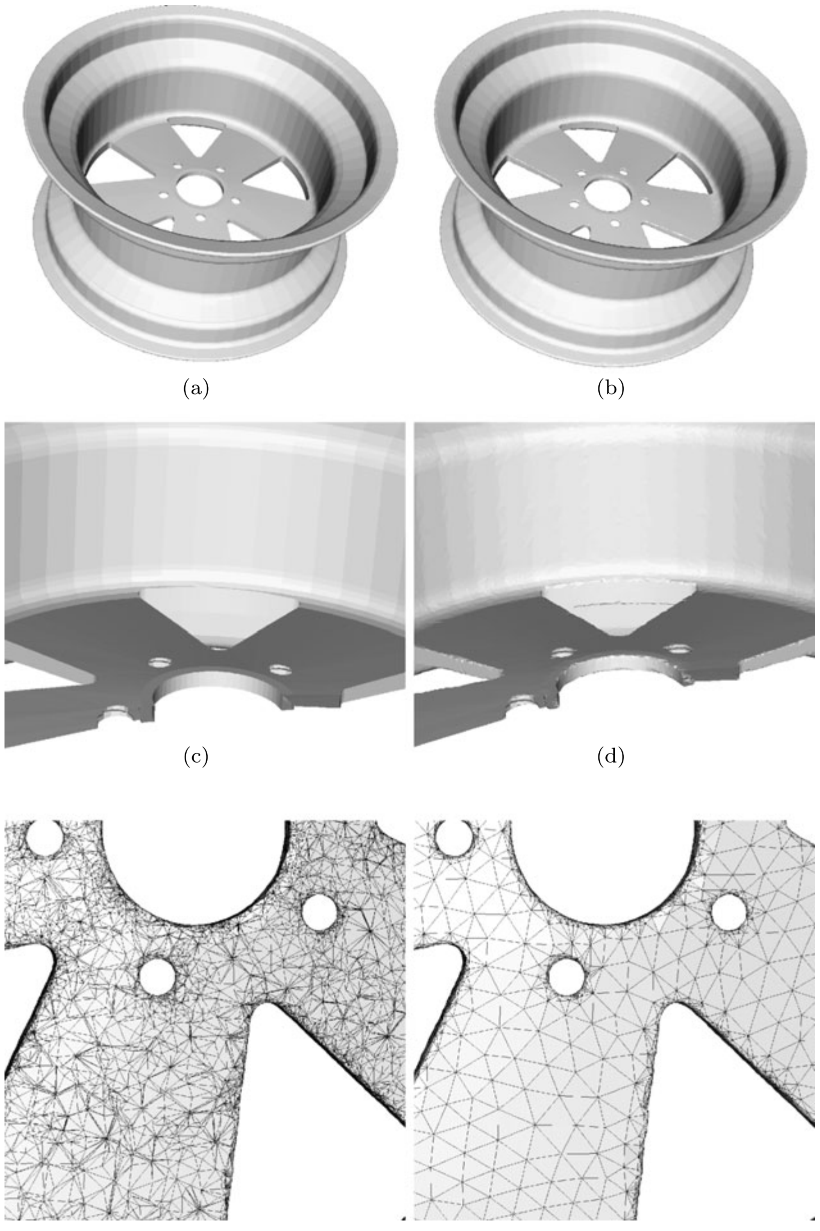

Fig. 10 Piecewise affine reconstruction of the wheel. (**a**) The original wheel (**b**) its reconstruction (**c**) a cut in the original wheel (**d**) a cut in the reconstruction (**e**) surface triangulation before remeshing (**f**) and after remeshing

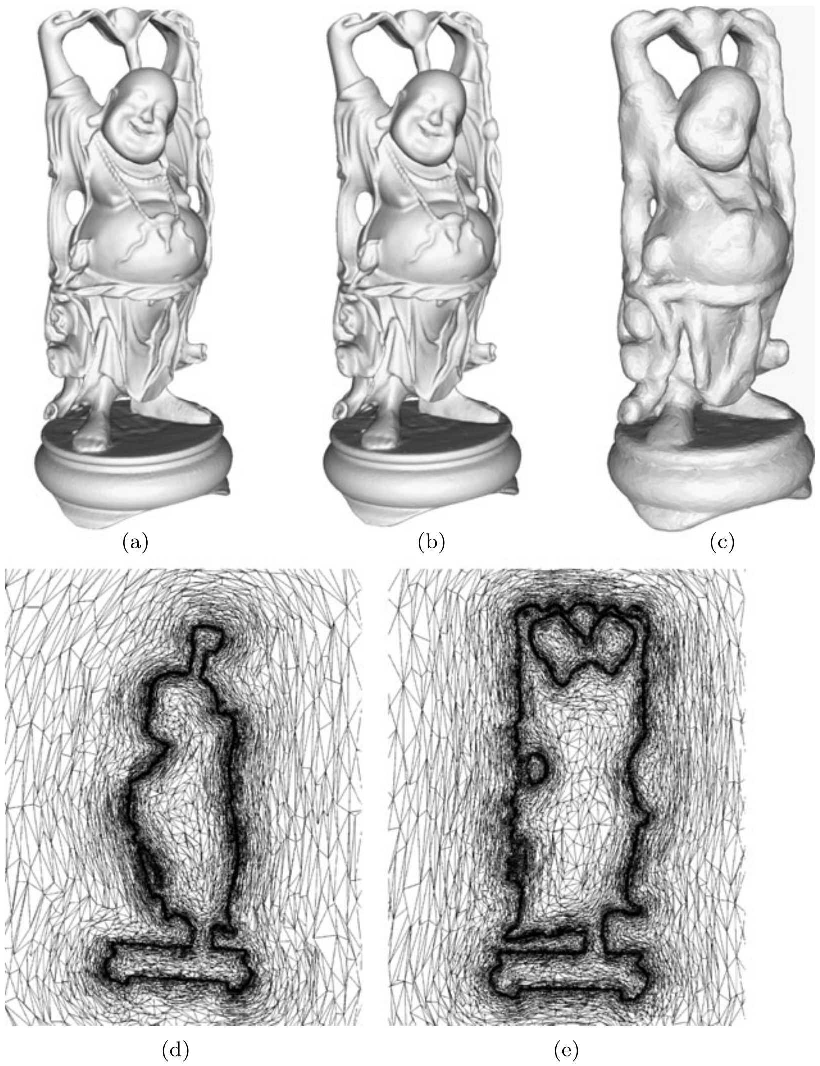

Fig. 11 Computation of the signed distance function to the Stanford "Happy Buddha"; (**a**) The initial Buddha (**b**) isovalue 0.001 of the computed signed distance function (**c**) isovalue 0.01 (**d**)–(**e**) Two cuts in the adapted mesh

dowed with the hyperbolic metric of the Poincaré half-plane: let Ω be a union a 3 disks, embedded in the half-plane $\mathbb{H} := \{(x, y) \in \mathbb{R}^2 | y > 0\}$ endowed with the so-called *Lobachevsky metric* defined by

$$\forall (x, y) \in \mathbb{H}, \quad M(x, y) := \frac{1}{y^2} I_2$$

where I_2 stands for the unitary matrix of dimension 2. Figure 9 then show some level sets of the signed distance function to Ω with respect to metric M.

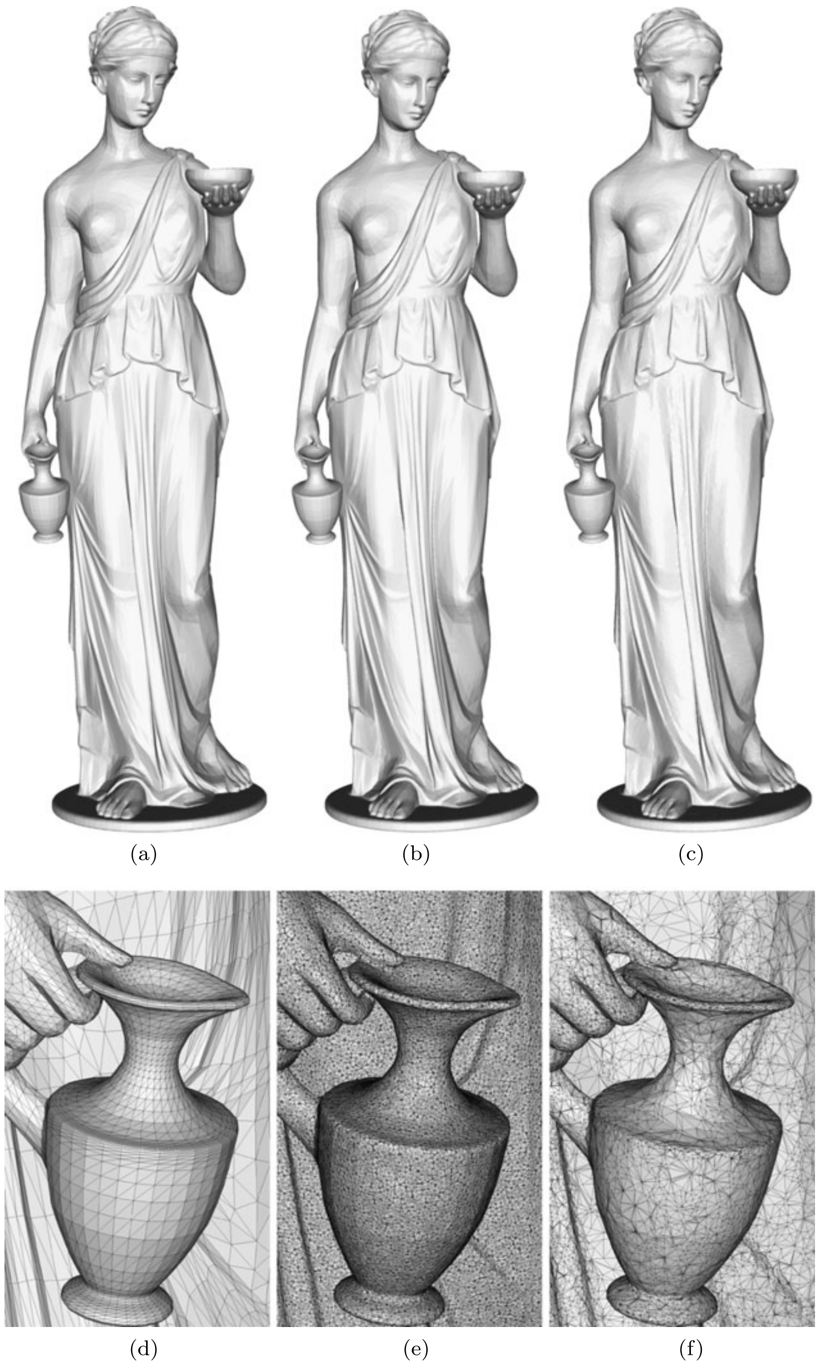

Fig. 12 Reconstruction of the "Venus": (**a**) The original Venus (**b**) Its reconstruction with isotropic mesh adaptation (3093941 surface triangles) (**c**) Its reconstruction with anisotropic mesh adaptation (300968 surface triangles) (**d**) zoom on the original Venus (**e**) zoom on its reconstruction with isotropic mesh adaptation (**f**) zoom on its reconstruction with anisotropic mesh adaptation

References

1. Alauzet, F., Frey, P.: Anisotropic mesh adaptation for CFD computations. Comput. Methods Appl. Mech. Eng. **194**, 5068–5082 (2005)
2. Alauzet, F., Frey, P.: Estimateur d' erreur géometrique et métriques anisotropes pour l' adaptation de maillage. Partie I: aspects théoriques. INRIA, Technical Report, p. 4759 (2003)
3. Anglada, M.V., Garcia, N.P., Crosa, P.B.: Directional adaptive surface triangulation. Comput. Aided Geom. Des. **16**, 107–126 (1999)
4. Apel, T.: Anisotropic Finite Elements: Local Estimates and Applications. Series of Advances in Numerical Mathematics. B.G. Teubner, Stuttgart, Leipzig (1999)
5. Aujol, J.F., Auber, G.: Signed distance functions and viscosity solutions of discontinuous Hamilton-Jacobi equations. INRIA, Technical Report, p. 4507 (2002)
6. Berger, M., Gostiaux, B.: Differential Geometry: Manifolds, Curves and Surfaces. Graduate Texts in Mathematics. Springer, Berlin (1987)
7. Bui, T.T.C., Frey, P., Maury, B.: A coupling strategy for solving two-fluid flows. Int. J. Numer. Methods Fluids (2010). doi:10.1002/fld.2730
8. Cheng, L.-T., Tsai, Y.-T.: Redistancing by flow of time dependent eikonal equation. J. Comput. Phys. **227**, 4002–4017 (2008)
9. Chopp, D.: Computing minimal surfaces via level-set curvature flow. J. Comput. Phys. **106**, 77–91 (1993)
10. Ciarlet, P.G.: The Finite Element Method for Elliptic Problems. North Holland, Amsterdam (1978)
11. Claisse, A., Frey, P.: Level set driven smooth curve approximation from unorganized or noisy point set. In: Proceedings ESAIM (2008)
12. Crandall, M.G., Ishii, H., Lions, P.L.: User's guide to viscosity solutions of second order partial differential equations. Bull. Am. Math. Soc. **27**, 1–67 (1992)
13. D'Azevedo, E.F., Simpson, R.B.: On optimal triangular meshes for minimizing the gradient error. Numer. Math. **59**, 321–348 (1991)
14. Delfour, M.C., Zolesio, J.-P.: Shapes and Geometries. SIAM, Philadelphia (2001)
15. Ducrot, V., Frey, P.: Contrôle de l'approximation géometrique d une interface par une métrique anisotrope. C. R. Acad. Sci., Ser. 1 Math. **345**, 537–542 (2007)
16. Evans, L.C.: Partial Differential Equations. American Mathematical Society, Providence (1997)
17. Frey, P.J., George, P.L.: Mesh Generation: Application to Finite Elements, 2nd edn. Wiley, New York (2008)
18. Dobrzynski, C., Frey, P.: Anisotropic Delaunay mesh adaptation for unsteady simulations. In: Proc. of the 17th IMR, pp. 177–194 (2008)
19. Fuhrmann, A., Sobottka, G., Gross, C.: Abstract distance fields for rapid collision detection in physically based modeling. In: Proceedings of International Conference Graphicon (2003)
20. Gomes, A.J.P., Voiculescu, I., Jorge, J., Wyvill, B., Gallsbraith, C.: Implicit Curves and Surfaces: Mathematics, Data Structures and Algorithms. Springer, Berlin (2009)
21. Guigue, P., Devillers, O.: Fast and robust triangle-triangle overlap test using orientation predicates. J. Graph. GPU Game Tools **8**, 25–42 (2003)
22. Vallet, M.G., Hecht, F., Mantel, B.: Anisotropic control of mesh generation based upon a Voronoi type method. In: Numerical Grid Generation in Computational Fluid Dynamics and Related Fields (1991)
23. Huang, W.: Metric tensors for anisotropic mesh generation. J. Comput. Phys. **204**, 633–665 (2005)
24. Ishii, H.: Existence and uniqueness of solutions of Hamilton-Jacobi equations. Funkc. Ekvacioj **29**, 167–188 (1986)
25. Jones, M.W.: 3D distance from a point to a triangle. Department of Computer Sciences, University of Wales Swansea, technical report (1995)
26. Kimmel, R., Sethian, J.A.: Computing geodesic paths on manifolds. Proc. Natl. Acad. Sci. USA **95**, 8431–8435 (1998)
27. Mantegazza, C., Mennucci, A.C.: Hamilton-Jacobi equations and distance functions on Riemannian manifolds. Appl. Math. Optim. **47**, 1–25 (2003)
28. Marchandise, E., Remacle, J.-F., Chevaugeon, N.: A quadrature free discontinuous Galerkin method for the level set equation. J. Comput. Phys. **212**, 338–357 (2005)
29. Mut, F., Buscaglia, G.C., Dari, E.A.: A new mass-conserving algorithm for level-set redistancing on unstructured meshes. Mec. Comput. **23**, 1659–1678 (2004)
30. Page, D.L., Sun, Y., Koschan, A.F., Paik, J., Abidi, M.A.: Normal vector voting: crease detection and curvature estimation on large, noisy meshes. Graph. Models **64**, 199–229 (2004)

31. Qian, J., Zhang, Y.T., Zhao, H.: Fast sweeping methods for Eikonal equations on triangular meshes. SIAM J. Numer. Anal. **45**, 83–107 (2007)
32. Osher, S.J., Fedkiw, R.: Level Set Methods and Dynamic Implicit Surfaces. Springer, Berlin (2002)
33. Osher, S.J., Sethian, J.A.: Fronts propagating with curvature-dependent speed: algorithms based on Hamilton–Jacobi formulations. J. Comput. Phys. **79**, 12–49 (1988)
34. Memoli, F., Sapiro, G.: Fast computation of weighted distance functions and geodesics on implicit hyper-surfaces. J. Comput. Phys. **173**, 730–764 (2001)
35. Sethian, J.A.: Fast marching methods. SIAM Rev. **41**, 199–235 (1999)
36. Sethian, J.A.: A fast marching method for monotonically advancing fronts. Proc. Natl. Acad. Sci. USA **93**, 1591–1595 (1996)
37. Sethian, J.A.: Level Set Methods and Fast Marching Methods: Evolving Interfaces in Computational Geometry, Fluid Mechanics, Computer Vision, and Materials Science. Cambridge University Press, Cambridge (1999)
38. Osher, S.J., Smereka, P., Sussman, M.: A level set approach for computing solutions to incompressible two-phase flow. J. Comput. Phys. **114**, 146–159 (1994)
39. Strain, J.: Fast tree-based redistancing for level set computations. J. Comput. Phys. **152**, 664–686 (1999)
40. Sussman, M., Fatemi, E.: An efficient, interface-preserving level set redistancing algorithm and its applications to interfacial incompressible fluid flow. SIAM J. Sci. Comput. **20**, 1165–1191 (1999)
41. Sussman, M., Fatemi, E., Smereka, P., Osher, S.: An improved level-set method for incompressible two-phase flows. Comput. Fluids **27**, 663–680 (1997)
42. Zhao, H.: A fast sweeping method for eikonal equations. Math. Comput. **74**, 603–627 (2005)
43. Zhao, H., Osher, S.J., Fedkiw, R.: Fast surface reconstruction using the level set method. In: Proceedings of IEEE Workshop on Variational and Level Set Methods in Computer Vision (2001)